Korean Journal of Geomatics
Vol. 2, No. 2 / December 2002
pp. 123~130

3-Dimensional Building Reconstruction with Airborne LiDAR Data

Dong-Cheon LEE*, Jae-Hong YOM, Jay-Hyoun KWON* and Gwang-Jae WE*****

Abstract

LiDAR (Light Detection And Ranging) system has a profound impact on geoinformatics. The laser mapping system is now recognized as being a viable system to produce the digital surface model rapidly and efficiently. Indeed the number of its applications and users has grown at a surprising rate in recent years. Interest is now focused on the reconstruction of buildings in urban areas from LiDAR data. Although with present technology objects can be extracted and reconstructed automatically using LiDAR data, the quality issue of the results is still major concern in terms of geometric accuracy. It would be enormously beneficial to the geoinformatics industry if geometrically accurate modeling of topographic surface including man-made objects could be produced automatically. The objectives of this study are to reconstruct buildings using airborne LiDAR data and to evaluate accuracy of the result. In these regards, firstly systematic errors involved with ALS (Airborne Laser Scanning) system are introduced. Secondly, the overall LiDAR data quality was estimated based on the ground check points, then classifying the laser points was performed. In this study, buildings were reconstructed from the classified as building laser point clouds. The most likely planar surfaces were estimated by the least-square method using the laser points classified as being planes.Intersecting lines of the planes were then computed and these were defined as the building boundaries. Finally, quality of the reconstructed building was evaluated.

Keywords : LiDAR, Laser Altimetry, Error Modeling, DEM, Surface Reconstruction

1. Introduction

Multi-sensor data become increasingly available from various systems. These data could be obtained from the optical imaging systems (*e.g.*, aerial photographs, satellite imagery, multi/hyper-spectral imagery) and non-optical systems (*e.g.*, LiDAR, SAR; Synthetic Aperture Radar, GPS; Global Positioning System, INS; Inertia Navigation System, satellite altimetry, and other data from microwave sensors). One of the systems that have a profound impact on geoinformatics community is laser (Light Amplification by Stimulated Emission of Radiation) scanning systems, so call 'LiDAR' system. The LiDAR system transmits laser out to target areas. The transmitted light interacts with and is changed by the surfaces of the targets. Some of the light is reflected and/or scattered back to the LiDAR instrument where the return signals are analyzed. The time for the light to travel out to the targets and return back to the LiDAR instrument is used to determine therange to the targets.

The first laser system implemented for photogrammetric and topographic mapping processes was laser APR (Airborne Profile Recorder) in early 1970's. At that time, however, the laser systems only provided auxiliary data for aerial triangulation and generating DEM (Digital Elevation Model). In early 1990's, the first airborne laser terrain mapping (ALTM) system was in operation. Currently, around 60 ALS systems are available in world wide such as NASA's ATM (Airborne Topographic Mapper), Optech and Leica-Helava laser scanning systems (Sizgoric, 2002). Spaceborne laser altimeters are in operation such as SLA (Shuttle Laser Altimeter), VCL (Vegetation Canopy LiDAR) and GLAS (Geosciences Laser Altimeter). Also topographic mapping of Mars is provided by NASA's Mars Orbiter Laser Altimeter (MOLA). Fig. 1 shows a relief-shaded color contour map generated

*Asst. Prof. Dept. of Geoinformation Engineering, Research Institute of Geoinformation & Geophysics, Sejong University (E-mail : dclee@sejong.ac.kr)
**Assc. Prof. Dept. of Geoinformation Engineering, Research Institute of Geoinformation & Geophysics, Sejong University
***Researcher, GIS Technology Research Institute, Hanjin Information Systems & Telecommunication

The manuscript for this paper was submitted for review on December 5, 2002.

by processing laser data that was acquired by Mars Orbiter Laser Altimeter (MOLA).

The major applications with laser scanning system are topographic mapping (*e.g.*, rapid DEM generation and topographic surface/object reconstruction), electrical transmission facility monitoring (*e.g.*, power line mapping, catenary modeling of wires, tower locations, and ground clearance), forestry (*e.g.*, tree height determination, and terrain modeling hidden beneath the forest canopy), wireless/mobile telecommunication (*e.g.*, urban canyon measurement, obstruction environment analysis, wave propagation modeling for the optimal antenna location simulation), costal engineering (*e.g.*, rapid survey of dynamic costal areas, coastal zone management, and analysis of post-storm survey), city modeling (*e.g.*, 3D virtual reality of urban areas, urban planning, and urban information system), natural disaster monitoring /managements (*e.g.*, flood management), and glacial region study (*e.g.*, sea-ice mapping and ice thickness measurement).

The processing of the ALS data consists of evaluation of data quality, grouping or classification of laser point clouds, segmentation, surface/object reconstruction, and analysis (Schenk *et al.*, 1999). One of the major issues to be considered in topographic mapping application of the ALS system is quality of the laser data in terms of point accuracy with error modeling. Schenk (2002) has intensively investigated and analyzed ALS errors and proposed an error modeling. State-of-the-art ALS systems have capability to produce elevation data with better than 15cm accuracy from an altitude of 1,200m (Friess, 2002). Referring to the rule of thumb for estimating height accuracy of bundle adjustment:

$$\sigma_Z = 0.03‰\ H \tag{1}$$

where H: Aircraft altitude.

In this study, the height accuracy provided by precise aerial triangulation is approximately 35cm with an aircraft altitude of 1,200m. However, current ALS systems hardly exceed flying height of 2,000m. Quality control issue in terms of ALS error modeling was described and building reconstruction by planar surface fitting with classified laser points by least-square method was proposed. Finally, the accuracy of the reconstructed buildings was evaluated by comparing aerial triangulation results that serve as reference data.

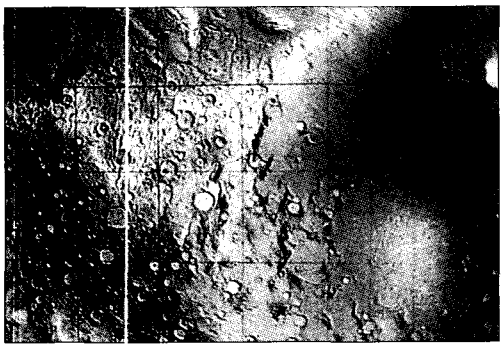

Fig. 1. Relief-shaded color contour map generated from Mars Orbiter Laser Altimeter (MOLA).

2. Systematic Errors in ALS

ALS systems consist of on-board GPS receiver, INS and laser scanner (Fig. 2). The major workflow of processing LiDAR data consists of sensor calibration, georeferencing, laser point cloud generation, classification and grouping (or segmentation) of the point clouds, filtering and quality control. However, there is no formal or standardized calibration procedures of the ALS systems available yet, in stead ad-hoc based calibration techniques have been implemented. Therefore, modeling systematic errors, design-independent calibration techniques, and analyzing independent verification method are key issues to obtain reliable data from ALS systems (Flood, 2001; Schenk, 2002).

In order to perform calibration of the ALS system, error sources and parameters are to be identified first then an appropriate error model has to be developed. The identifiable systematic errors (*i.e.*, sensor related errors) eventually being removed are described as follows (Schenk, 2001):

- Range error: Error in range measurement.
- Scan angle errors: Error caused by spatial direction of the laser beam consists of index error, swath angle error and scan plane error.

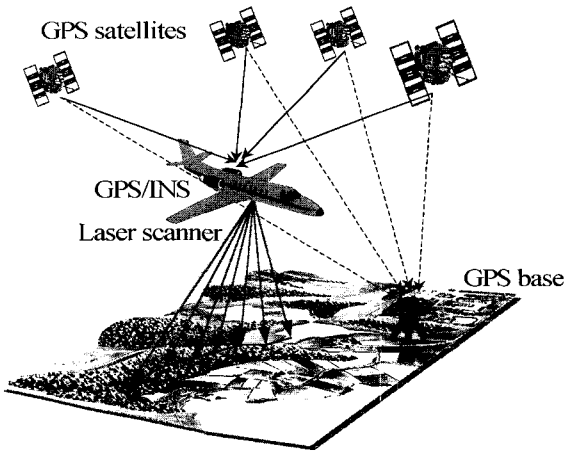

Fig. 2. Airborne laser scanning system.

- Mounting errors: Error caused by laser scanner mounting errors (*i.e.*, transformation of laser scanner coordinate system to INS system, and GPS mounting errors (*i.e.*, translation between INS coordinate system and GPS receiver system).
- INS errors: Errors caused by INS initialization, misalignment, and gyro drifts.
- GPS error: Errors caused by troposphereic/ ionospheric effects and multipath of the GPS signal.
- Geoid normal error: Errors caused by transformation from the INS coordinate system to reference system (*i.e.*, WGS84).
- Time bias: ALS system consists of independently operating components (*i.e.*, GPS, IMU (Inertial Measurement Unit) and laser scanner) in terms of different sampling frequency. These lead synchronization and interpolation errors.

Other non-sensor related errors are explained by function of the surface topography interacts with laser signal that are difficult to model. The remaining random errors are to be handled statistically. In general, accuracy of the LiDAR is defined by measure of the nearness of the computed laser point position to the real (or true) measured laser point position. The accuracy is expressed as standard deviations of the laser point coordinates (*i.e.*, error propagation). The major factors affecting the quality of the LiDAR are sensor orientation (*i.e.*, laser firing position and laser beam attitude) and scanner angle. Other non-sensor related factors are distribution of laser points, processing algorithms, and extracted features.

3. Study Site and Quality of the LiDAR Data

LiDAR data was collected over Chung Ju city area (Fig. 3) by Optech ALTM1020 system in January, 2002. The average point density was 2.6 pts/m^2, that yields average point spacing of 0.4m, with flying height of 1,000 m and aircraft speed of 180 km/h. The scan width was 450m and the overlap was 87%. In order to evaluate overall quality of the LiDAR data, 26 check points on the ground were compared to LiDAR data. The check points were obtained by fast-static GPS surveying for 30 minutes for each point. Most of the check points were located in the flat areas in order to reduce interpolation errors of LiDAR points. Table 1 shows the GPS surveying results and corresponding LiDAR point elevations that were derived by linear interpolation. It should be noted that the coordinates of the GPS surveying are represented in TM coordinate system (East, North) and elevation (H) after applying the transformation from the WGS84 coordinate system to TM (Transverse Mercator) coordinate system. For transformation between above two coordinate systems can be found in Snyder (1987).

The overall accuracy of the LiDAR data was estimated by computing the root-mean-square-error of elevations ($RMSE_Z$) implemented by National Standard for Spatial Data Accuracy (NSSDA):

$$RMSE_Z = \sqrt{\frac{\sum (Z_{CP} - Z_{LP})^2}{n}} \quad (2)$$

where Z_{CP}: Elevations of the check points Z_{LP}: Eleva-

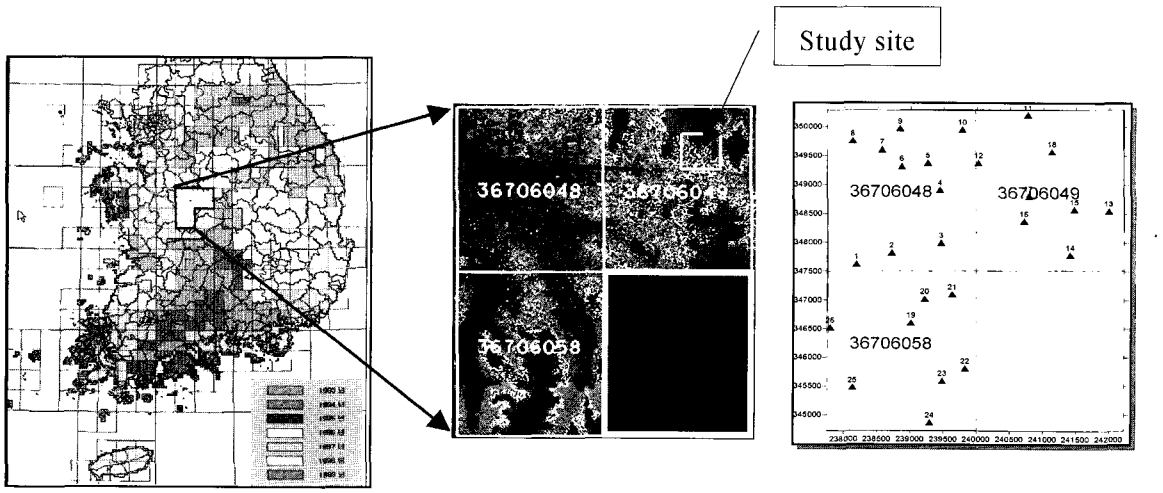

Fig. 3. Study site and distribution of the ground check points (Numbers on each quadrant indicate index number of the 1/5,000 aerial photographs).

Table 1. Comparison between LiDAR data and GPS surveying for the ground check points

(Courtesy Korea National Geography Institute)

Point ID	Coordinates from GPS surveying (m)			Elevation from ALS (m)	Difference (m)
	X	Y	Z	Z_{LiDAR}	Z_{GPS} - Z_{LiDAR}
1	238182.73	347608.83	43.33	43.32	0.01
2	238712.75	347801.50	57.21	57.23	-0.02
3	239458.15	347982.41	44.38	44.27	0.11
4	239442.36	348890.89	48.90	48.81	0.09
5	239260.89	349359.09	45.96	45.83	0.13
6	238868.63	349300.46	40.81	40.82	-0.01
7	238569.21	349588.75	45.89	45.83	0.06
8	238124.78	349737.39	46.68	46.77	-0.09
9	238836.47	349951.55	59.88	59.93	-0.05
10	239777.32	349933.31	61.61	61.62	-0.01
11	240767.60	350185.10	64.83	64.97	-0.14
12	240021.65	349361.27	57.43	57.45	-0.02
13	241987.14	348531.43	69.89	69.88	0.01
14	241406.90	347766.62	71.15	71.10	0.06
15	241464.49	348558.91	68.30	69.01	-0.71
16	240708.42	348353.83	60.75	60.74	0.01
17	240779.73	348780.24	62.93	62.91	0.02
18	241131.02	349552.97	68.93	68.96	-0.03
19	239005.89	346588.45	61.47	61.47	0.00
20	239213.75	347005.69	54.73	54.62	0.11
21	239627.63	347083.56	54.39	54.39	0.00
22	239825.18	345790.84	56.28	56.22	0.06
23	239479.59	345576.67	59.18	59.27	-0.09
24	239292.53	344852.99	59.42	59.31	0.11
25	238130.23	345459.72	52.12	52.43	-0.31
26	237789.72	346502.43	48.80	49.01	-0.21
				RMSE	0.29

Note: X-,Y- and Z-coordinate denotes Easting, Northing in TM coordinate system and elevation, respectively.

tions of the laser points, and *n*: Number of points. RMSE of the LiDAR elevation was 0.29m. The error range of the elevation (*i.e.*, accuracy) with 95% uncertainty level is then estimated as ± 1.96 *RMSEz* (so call "*two-sigma error*"). Therefore, the comparison between reference data and LiDAR data suggests that there is no significant systematic bias in the LiDAR data.

4. Building Reconstruction with LiDAR Data

Even though LiDAR data provides accurate position information with high spatial frequency they do not provide well define object boundaries because of lack of thematic information (Ackermann, 1999; McIntosh *et al.*, 1999). Fig. 4 shows discrepancy between physical and LiDAR driven building boundaries.

Therefore, it is difficult task to determine the physical object boundaries precisely with laser points only without additional information such as imagery. There are two ways to determine object boundary by registering laser points onto images: (1) Registering laser points onto orthoimagery. (2) Projecting laser points back to left and right images of the stereopair (Csatho *et al.*, 1999). However, both methods require intensive post-processing procedure and external data

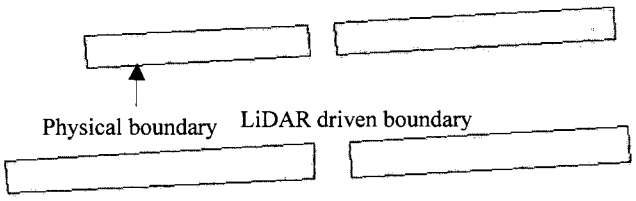

Fig. 4. Comparison between physical building boundaries and LiDAR driven building boundaries.

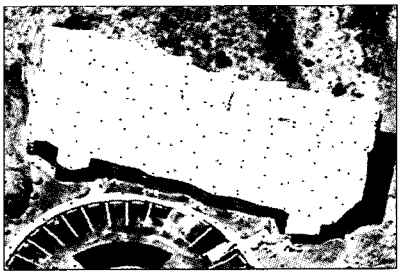

Fig. 5. Laser points registered on the orthoimage.

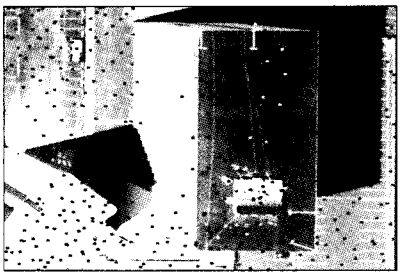

(a) Left image

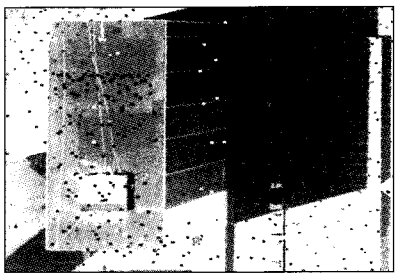

(b) Right image

Fig. 6. Laser points projected back to the stereopair by collinearity equations with exterior parameters.

set including digital elevation model (DEM), and orientation parameters of the stereo images. Fig. 5 and 6 show the laser points registered on the orthoimage and the stereopair, respectively using data set provided by ISPRS Working Group III/5. The data set comprises aerial photographs, LiDAR data acquired by NASA's ATM, multispectral and hyperspectral imagery over Ocean City, Maryland, USA. Readers could find more detail information about the data set in Csatho (1999), Schenk (1999), and Lee (2001).

5. Planar Surface Fitting with the Laser Points by Least-Square Method

Laser point clouds were classified as buildings, vegetation, and ground by TerraScan software. The points classified into buildings were analyzed since the purpose of this study is to reconstruct building. The major parameters for classifying buildings are height and size. Fig. 7 depicts laser point clouds of buildings in the study site.

The planar surface defined by the laser points is de fined as:

$$Z_i = aX_i + bY_i + c + e_i \tag{3}$$

where (X_i , Y_i , Z_i): Coordinates of the laser points on a plane, e_i: Errors, and *a, b, c*: Plane parameters. The plane parameters were determined by least-square estimation based on Gauss-Markov model as:

$$y = A\xi + e, \quad e \sim (0,\ \sigma_o^2 P) \tag{4}$$

where $y = \begin{bmatrix} Z_1 \\ Z_2 \\ \cdots \\ Z_n \end{bmatrix}$, $A = \begin{bmatrix} X_1 & Y_1 & 1 \\ X_2 & Y_2 & 1 \\ \cdots & \cdots & \cdots \\ X_n & Y_n & 1 \end{bmatrix}$, $\xi = \begin{bmatrix} a \\ b \\ c \end{bmatrix}$,

$e = \begin{bmatrix} e_1 \\ e_2 \\ \cdots \\ e_n \end{bmatrix}$, with σ_o^2: Variance component, and P: Weight matrix ($P = I$). The estimation of the parameter vector is determined by:

$$\hat{\xi} = (A^T PA)^{-1} A^T Py \tag{5}$$

Intersections of the adjacent surfaces determined by

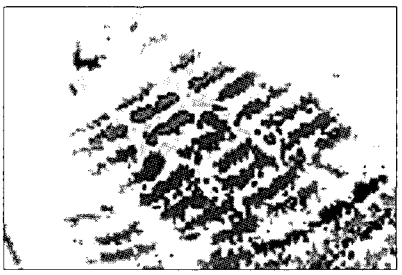

Fig. 7. Laser point clouds classified as buildings.

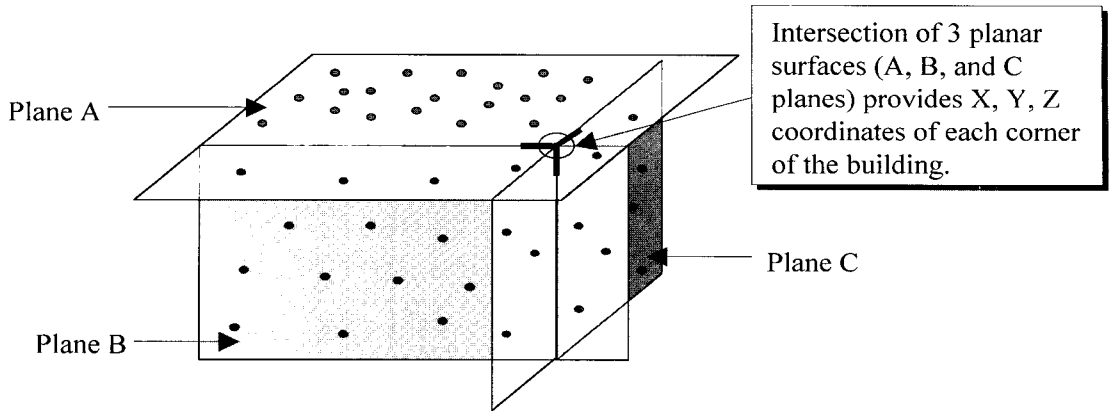

Fig. 8. Intersections of the planes (i.e., A: roof top, B and C: side walls) determined by planar surface fitting with least-square method provide 3D coordinates along the building boundary (Solid circles represent laser points).

the laser points on the side walls (*e.g.*, plane B and plane C in Fig. 8) provide planimetric coordinates (*i.e.*, X, Y) of the building corners. On the other hand, intersection of the pairs of adjacent side walls and roof top (*e.g.*, intersection of plane A, plane B and plane C in Fig. 8) provides height information (*i.e.*, Z) of the building corners.

The coordinates of each corner of the building are determined by using three planar surface equations that define a corner of the building as follows:

$$\begin{bmatrix} c_1 \\ c_2 \\ c_3 \end{bmatrix} = \begin{bmatrix} -a & -b_1 & 1 \\ -a_2 & -b_2 & 1 \\ -a_3 & -b_3 & 1 \end{bmatrix} \begin{bmatrix} X \\ Y \\ Z \end{bmatrix} \tag{6}$$

where $[X, Y, Z]^T$: Coordinates of a corner, and a_1, ..., c_3: Plane parameters determined by Eq. 5.

6. Experimental Results and Analysis

Fig. 9 and Fig. 10 show actual building on an aerial photograph and distribution of the laser points, respectively. Fig. 11 shows reconstructed study site and test building for evaluation of the accuracy.

The typical ways to evaluate quality of the results

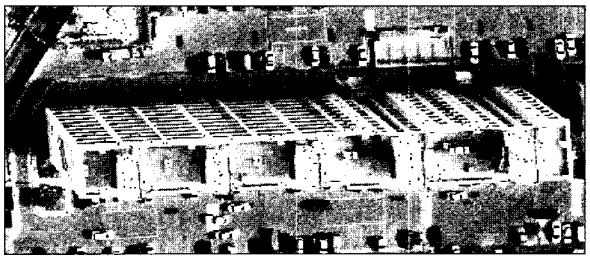

Fig. 9. An aerial photograph of the building.

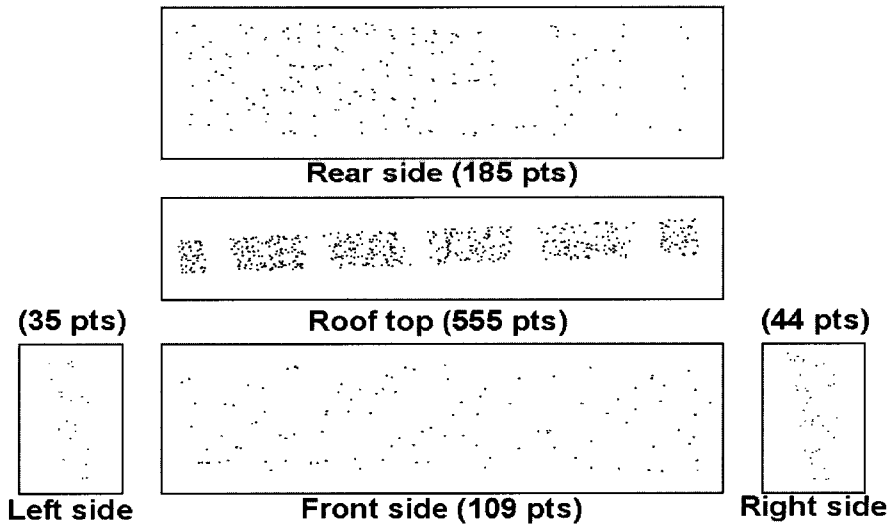

Fig. 10. Distribution of the laser points on each side of the building.

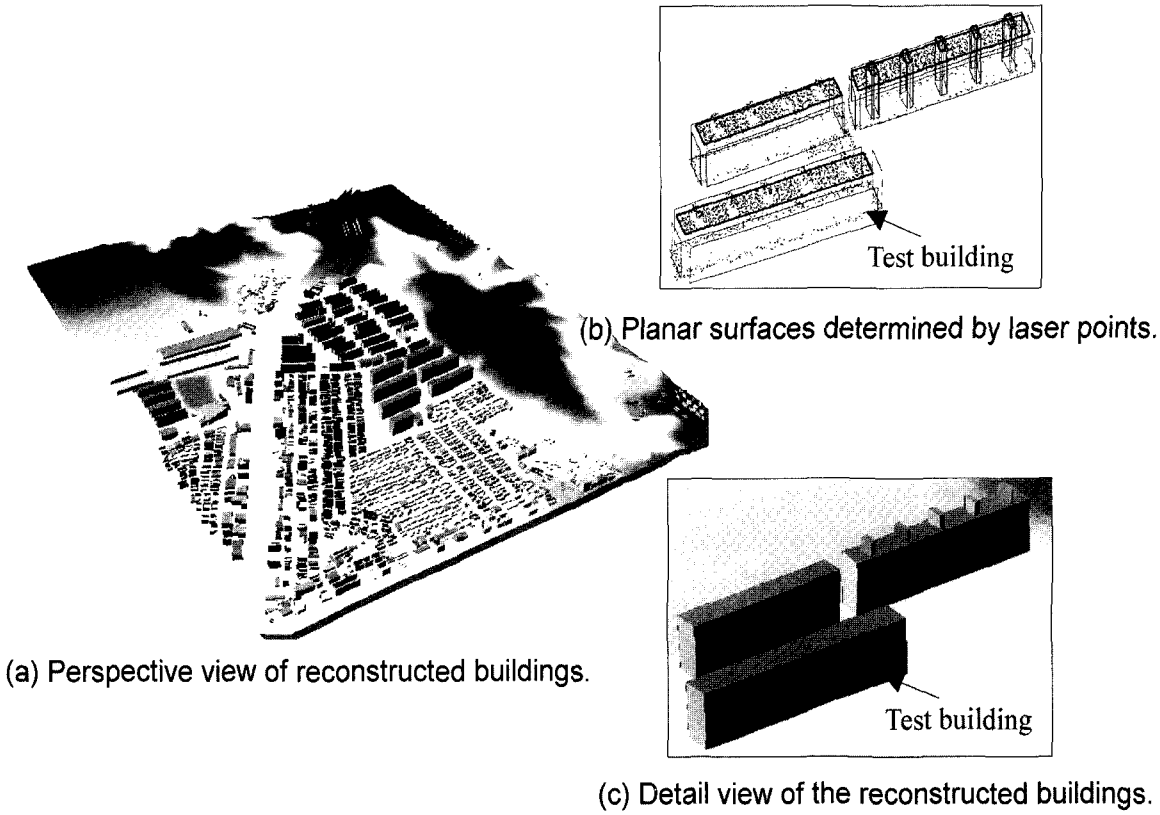

Fig. 11. 3D reconstruction of the ground surface and buildings with ALS data.

Table 2. Comparison between photogrammetry and LiDAR result at the corner of the building

		X(m)	⊿X(m)	Y(m)	⊿Y(m)	Z(m)	⊿Z(m)
Corner 1	Photo	241722.70	0.36	349583.53	0.70	101.80	-0.07
	LiDAR	241722.34		349582.83		101.87	
Corner 2	Photo	241722.11	0.42	349592.86	-0.56	101.80	0.38
	LiDAR	241721.69		349593.42		101.42	
Corner 3	Photo	241790.39	0.37	349596.54	-0.76	101.80	0.93
	LiDAR	241790.02		349597.30		100.87	
Corner 4	Photo	241790.91	0.16	349587.29	0.75	101.80	0.09
	LiDAR	241791.07		349586.54		101.71	

from LiDAR data are visual inspection, measurement in strip overlap, comparison to reference height data, or comparison to maps. In this study, the coordinates of corner of the reconstructed buildings were compared to stereo compiled result after bundle adjustment. The results are described in Table 2.

The discrepancy in Y-coordinates is larger than in X-coordinates because the planes determined with laser points on the front and rear side walls are not geometrically homogeneously distributed due to the terraces and windows on those walls while the left and right walls are flat surfaces. Comparing the result from building reconstruction and the overall quality of the LiDAR data, the reconstruction accuracy was lower because the wave forms of the laser are more complicated in the residential areas with tall buildings than in the flat open areas where the ground check points are located.

The elevator towers could not direct reconstructed because there were not sufficient laser points on the side surfaces of the towers. In order to reconstruct buildings successfully in the urban areas where occluding areas cause the serious problem, the flight plan should be established carefully before hand including flying height and direction, overlap, scan rate and so

on. Reconstruction of the complicated shape of the buildings depends on the quality, number and distribution of the laser points, and segmentation of the laser point clouds.

7. Conclusions

In this study, three-dimensional building reconstruction was performed with airborne LiDAR data for urban area. Planar surfaces were generated for building reconstruction by least-square method then the accuracy of the result was compared with stereo compiled result. The building reconstruction approach presented this study method does not require additional information such as imagery but classification and grouping process of the laser point clouds. Y-coordinates have lower accuracy due to structural characteristics of the building. However, the accuracy of the building reconstruction has relative sense because there was no absolute reference surface available to evaluate LiDAR data. Based on the experiment following conclusions are drawn:

- Geometrical grouping of the LiDAR data provides meaningful information about the objects
- Accurately defined surfaces play an important role for mapping applications with LIDAR data
- Laser returns reflected from the sides of buildings are useful in the determination of the building boundaries that eventually provide valuable information for object reconstruction.
- However, at least three laser points should be on the side walls to reconstruct buildings with proposed method therefore, it might be not appropriate for buildings with low height.
- For the future work, to improve classification of the laser points, appropriate segmentation techniques (*e.g.*, Vosselman and Dijkman, 2001; Lee and Schenk, 2001) of the point clouds are suggested to be implemented.

Acknowledgments

This study was supported by the Korea Science & Engineering Foundation (Grant No. R01-2001-00073-0). LiDAR, GPS surveying data and aerial photographs were provided by the Korea National Geography Institute.

References

1. Ackermann, F. (1999). "Airborne Laser scanning: Present Status and Future Expectations." *ISPRS Journal of Photogrammetry and Remote Sensing*, Vol. 54, No. 1, pp. 64-67.
2. Csatho, B., Schenk, T., Lee, D. C. and Filin, S. (1999). "Inclusion of Multispectral Data into Object Recognition." *International Archives of Photogrammetry and Remote Sensing, Balladolid, Spain*, Vol. 32, Part 7-4-3 W6, pp. 53-60.
3. Flood, M. (2001). "LIDAR Activities and Research Priorities in the Commercial Sector." *International Archives of Photogrammetry and Remote Sensing*, Annapolis, MD, USA, Vol. 34, Part 3 W4, pp. 3-7.
4. Friess, P. (2002). "Tutorial on Laser Altimetry – Data Acquisition." *The 2nd Duane C. Brown International Summer School in Geomatics*, Columbus, OH, USA.
5. Lee, D. C. and Schenk, T. (2001). "A Study on Accuracy Analysis Methods of Airborne Laser Scanning System for Mapping Applications." *KSCE Journal of Civil Engineering*, Vol. 21, No. 2-D, pp. 209-217.
6. Lee, D. C., Yom, J. H., Kim, J. W., Kwon, J. H., We, K. J. and Kim, D. I. (2002). "Evaluation of LIDAR Data for Digital Mapping." *The 3rd International LIDAR Workshop*, Columbus, OH, USA, in press.
7. Lee, I.P. and Schenk, T. (2002). "3D Perceptual Organization from Laser Altimetry Data." *International Archives of Photogrammetry and Remote Sensing*, Annapolis, MD, USA, Vol. 34, Part 3 W4, pp. 27-28.
8. McIntosh, K., Krupnik, A. and Schenk, T. (1999). "Utilizing Airborne Laser Altimetry for the Improvement of Automatically Generated DEMs over Ubarn Areas." *International Archives of Photogrammetry and Remote Sensing*, La Jolla, CA, USA, Vol. 32, Part 3 W14,, pp. 89-94.
9. Schenk T. (2001). "Modeling and Analyzing Systematic Errors in Airborne Laser Scanners." Technical Note No. 19, Dept. of Civil and Environmental Engineering & Geodetic Science, The Ohio State University, Columbus, OH, USA.
10. Schenk, T., Csatho, B. and Lee, D. C. (1999). "Quality Control Issues of Airborne Laser Ranging Data and Accuracy Study in Urban Area." *International Archives of Photogrammetry and Remote Sensing*, La Jolla, CA, USA, Vol. 32, Part 3 W14, pp. 101-108.
11. Sizgoric, S. (2002). "Tutorial on Laser Altimetry - Airborne Laser Scanning: Introduction and General Overview." *The 2nd Duane C. Brown International Summer School in Geomatics*, Columbus, OH, USA.
12. Snyder, J. (1987). Map Projections — A Working Manual. U.S. Geological Survey Professional Paper 1395, U.S. Geological Survey, Washington, D.C.
13. Vosselman, G. and Dijkman, S. (2001). "3D Building Reconstruction from Point Clouds and Ground Plans." *International Archives of Photogrammetry and Remote Sensing*, Annapolis, MD, USA, Vol. 34, Part 3 W4, pp. 19-22.